

Level dynamics and avoided level crossings in driven disordered quantum dots

András Grabarits^{1,2}

¹*Department of Theoretical Physics, Institute of Physics,
Budapest University of Technology and Economics, Műegyetem rkp. 3., H-1111 Budapest, Hungary*

²*MTA-BME Quantum Dynamics and Correlations Research Group,
Budapest University of Technology and Economics, Műegyetem rkp. 3., H-1111 Budapest, Hungary*

The statistical properties of the dynamics of energy levels are investigated in the case of two-dimensional disordered quantum dot models with nearest neighbor hopping subjected to external time-dependent perturbations. While in the first model the external drivings are realized by a continuous variation of the on-site energies, in the second one it is generated by deformations of a parabolic potential. We concentrate on the distribution of the spacing, velocity and curvature of the energy levels and on the statistics of the avoided level crossings. Our findings show that for both models, albeit under slightly different conditions, the statistical properties of these quantities are in good agreement with those predicted by Random Matrix Theory (RMT) for the Gaussian Orthogonal, Unitary and Symplectic ensembles. We also provide analytic results on the disorder and system size dependence of the typical magnitudes of the velocities, curvatures of energy levels, and of the gaps and the asymptotic slopes of the anticrossings. Our results can be verified experimentally by measurements of single-particle energy spectra in quantum dots.

I. INTRODUCTION

The spectra of complex, interacting many-body systems can be considered up to a large extent indeterministic, for which Random Matrix Theory (RMT) has proven to provide an accurate statistical description, relying only on the fundamental symmetries of the system and completely neglecting the microscopical details of the individual energy eigenstates [1–5]. While its applicability to the spectrum of disordered tight binding models has been the subject of many studies [6–10], the statistical behavior of motion of energy levels and its connection to RMT still raises many exciting unanswered questions. Urged by the swift experimental developments exploring non-equilibrium phenomena in the nanoscale regime, considerable theoretical attention is being paid to the response properties of disordered quantum dots to time-dependent perturbations. The effects of external drivings manifest themselves, among others, in the movements of energy levels, which in turn provide information about the changes of the physical quantities in the system induced during the non-equilibrium process.

One of the earliest approaches to study disordered systems is provided by the statistics of difference of adjacent energy levels. First of all, as was proposed in Ref. 11, levels repelling each other, characteristic for RMT, correspond to classically chaotic nature and follow the celebrated Wigner Dyson statistics [12], while regular motion implies Poissonian statistics. In addition, level spacing statistics also provides an ideal testbed to study localization properties of single particle states. In 3 dimensions RMT-like behavior is observed for states with localization lengths much larger than the system size and for delocalized states, while Anderson localized states with localization length shorter than the system size exhibit Poissonian level statistics and intermediate statistics were observed at the metal insulator transi-

tion [6, 13, 14]. A different picture emerges, however, in 2 dimensions as for spinless disordered tight binding models RMT-like behavior is only observed for states with localization length sufficiently exceeding the size of the system for both unit and random phase hopping terms (systems in the presence and absence of time-reversal symmetry, respectively) [7, 10, 15]. Furthermore, introducing also spin degrees of freedom and random spin-orbit couplings, as was thoroughly studied in Refs. 8, 16–19, truly extended states appear below a critical disorder value. Further works tested the validity of the Wigner statistics in various fields ranging from the early studies of Coloumb blockade [7] and conductance peak spacings [20] through the effects of Aharonov-Bohm flux piercing through disordered samples [21, 22], kicked one-dimensional systems [23] to the current investigation of interacting spin systems [24–27], finite range Coulomb gas models [28, 29], and open chaotic systems realised in microwave cavities [30].

Level spacing statistics, however, provides no information about responses to time-dependent perturbations. A large amount of non-equilibrium phenomena in disordered systems induced by external drivings can be addressed by the investigation of the motion of energy levels [31]. Level dynamics of classically chaotic systems was first formulated in the pioneering works of Refs. 32 and 33 exhibiting similar statistical behavior as the spectra of the proper Gaussian random matrix ensembles. With an appropriate parametric evolution of the $H(\lambda)$ disordered Hamiltonian with λ promoted to fictitious time, derivatives of energy levels reveal most of the non-equilibrium properties of driven systems. Of central interest are the first and second derivatives commonly referred to as level velocity and level curvature, $v_n = dE_n/d\lambda$, $K_n = d^2E_n/d\lambda^2$, respectively, providing information about conductance fluctuations and characterizing the sensitivity of energy levels to changing

boundaries in metallic samples [34–36]

While the RMT levels exhibit Gaussian velocity statistics exact curvature distributions resisted evaluation for quite a long time. The first analytical predictions for the tail of the curvature statistics were provided by various authors in Refs. 37–39 along with Simons and Altshuler discussing the universal features of the curvature statistics and velocity correlations in Refs. 40–42. Finally von Oppen and Fyodorov in Refs. 43–46 gave exact analytical expressions in the case of random matrices and metallic samples pierced through by an Aharonov-Bohm flux.

Velocity and curvature statistics constituting an intense area of research have been investigated over the years mostly in systems in the presence of a magnetic field [47, 48], in chaotic, irregularly shaped billiards with changing boundaries [49–54], and quantum systems with twisted boundary conditions [9, 55–58] or in periodically kicked one-dimensional systems [57, 59], while recent studies considered disordered interacting many-body systems [60–62].

A further striking feature in the course of parametric evolution of disordered systems is the formation of the avoided level crossings. In the seminal work of Wigner[63], it was argued that the levels of $H(\lambda)$ without any particular symmetries may reach close to each other at some λ_0 value but finally avoid true crossing points. Apart from providing an ideal testbed to study the degree of emerging chaos in the classical counterparts of quantum systems [64–68], avoided level crossings have a dramatic impact on the conditions of adiabatic time evolution in driven disordered systems. Following the common approximate expression around the closest approach of λ_0 ,

$$E_{n+1}(\lambda) - E_n(\lambda) \approx \sqrt{\Delta^2 + \gamma^2(\lambda - \lambda_0)^2}, \quad (1)$$

even for slowly varying $\lambda = \lambda(t)$ driving protocols adiabaticity can be violated via Landau-Zener (LZ) transitions with probability $\exp(-\frac{\pi}{2} \frac{\Delta^2}{\gamma\lambda})$ [69, 70] with Δ and γ being the smallest level distance (gap) and asymptotic slope, respectively. While pioneering studies on the LZ parameter statistics and their impact on non-equilibrium dynamics in random matrix ensembles were provided by Wilkinson in Refs. 71 and 72, their strong connection to classical diffusion processes and energy dissipation was established in Refs. 73–78.

The role of the avoided level crossings were studied in further exciting phenomena such as dynamical tunneling [79–82], relations to the famous Lyapunov exponents [83] or transitions from regular to chaotic regimes in classical systems [84, 85]. Similarly to level response investigations, LZ parameter statistics were compared to the RMT results in quantum billiards, kicked tops [86–90] and in disordered systems with Rashba and spin-forbit interactions [91, 92].

In spite of these extensive progresses, in most cases level dynamics were generated by magnetic fields and changing boundaries in microwave cavities or in chaotic

billiards not considering the possibility either of spin degrees of freedom or of different driving mechanisms such as deformations of a confining potential which could open new perspectives for experimental realizations. Furthermore, neither LZ parameter statistics nor level dynamics were investigated in two-dimensional systems with random magnetic fields or spin-orbit couplings (GUE, GSE symmetry class, respectively). In this paper we fill this gap by studying various aspects of level dynamics in two-dimensional disordered tight binding models with different driving protocols feasible for experimental realization in the case of all the *three* symmetry classes.

The paper is organized as follows. In Sec. II we present the two two-dimensional disordered quantum dot models. In Sec. III we show the agreement and argue for the differences of level spacing, level velocity and level curvature statistics compared to the RMT results and discuss their size and disorder dependences. In Sec. IV we show the agreement of the avoided level crossing parameters' distributions between RMT and the investigated models and also discuss their parameter dependences and their impacts on slowly driven systems.

II. THEORETICAL FRAMEWORK

Before turning to the detailed description of our results we briefly summarize the basic features of RMT. Random Gaussian matrices mainly divide into 3 classes according to their underlying symmetries, spinless systems with and without time-reversal symmetry described by real symmetric (GOE) and complex hermitian matrices (GUE) and spin one-half systems with time-reversal symmetry with quaternion valued hermitian matrices (GSE), respectively. The distribution of matrix elements for the above classes is given by

$$\mathcal{P}(H) \propto e^{-\frac{\beta N}{4J^2} \text{Tr}(HH^\dagger)} \quad (2)$$

with J fixing the energy scale and $\beta = 1, 2, 4$ denoting the number of independent real variables of each matrix element for GOE, GUE and GSE, respectively. Neighboring energies exhibit level repulsion as the distribution of their difference in the middle of the spectrum follows the celebrated Wigner-Dyson statistics [12],

$$P_{\text{level},\beta} \sim \Delta^\beta e^{-C_\beta \Delta^2} \quad (3)$$

with $C_\beta = \frac{\pi}{4}, \frac{4}{\pi}, \frac{64}{9\pi}$, implying $P_{\text{level},\beta}(\Delta) \sim \Delta^\beta$ for $\Delta = 0$. Following the works [72, 93], we choose the parametric evolution

$$H(\lambda) = H_i \cos \lambda + H_f \sin \lambda \quad (4)$$

with H_i and H_f being two independent random matrices drawn from the same ensemble and which ensures identical distribution of matrix elements at any value of λ . We

use this protocol to compare the statistical properties of level spacing, velocity, curvature and the Landau-Zener parameters to those obtained in the disordered quantum dot models. In particular, we consider the following model on a $L \times L$ square lattice ('on-site model'):

$$H_{\text{on-site}}(\lambda) = -J \sum_{\mathbf{r}, \delta, \alpha, \alpha'} t_{\mathbf{r}, \delta, \alpha, \alpha'} |\mathbf{r} + \delta, \alpha\rangle \langle \mathbf{r}, \alpha'| + \sum_{\mathbf{r}, \alpha} \epsilon_{\mathbf{r}, \lambda} |\mathbf{r}, \alpha\rangle \langle \mathbf{r}, \alpha| + \text{h. c.}, \quad (5)$$

where J sets the energy scale, $|\mathbf{r}, \alpha\rangle$ and $|\mathbf{r} + \delta, \alpha\rangle$ denote coordinate and spin eigenstates at lattice site \mathbf{r} and spin state α , respectively, and δ points to the nearest neighbors. For the spinless case, choosing unit hoppings $t_{\mathbf{r}, \delta} = 1$ GOE-like behavior, while for random phase hopping terms, $t_{\mathbf{r}, \delta} = e^{i\varphi_{\mathbf{r}, \delta}}$, with $\varphi_{\mathbf{r}, \delta}$ being uniformly and independently distributed in the interval $[-\pi, \pi]$, statistical properties similar to GUE are expected. For spin one-half systems with time-reversal symmetry, the appropriate choice, $t_{\mathbf{r}, \delta, \alpha, \alpha'} = (\mathbb{I} + \mu \boldsymbol{\sigma} \boldsymbol{\varphi}_{\mathbf{r}, \delta})_{\alpha, \alpha'}$ with μ denoting the strength of the spin-orbit coupling, leads to an energy spectrum characteristic for the GSE ensemble. Here $\boldsymbol{\varphi}_{\mathbf{r}, \delta}$ is a 3-component vector with independent random variables distributed uniformly on $[-1/2, 1/2]$ at each lattice site for all nearest neighbors, $\boldsymbol{\sigma}$ denotes the vector composed of the Pauli matrices and we chose, following Ref. 8, $\mu = 2$ for the strength of the spin-orbit coupling. Evolution in parameter space is realized by the protocol $\epsilon_{\mathbf{r}, \lambda} = \epsilon_{\mathbf{r}, i} \cos(\lambda) + \epsilon_{\mathbf{r}, f} \sin(\lambda)$ starting from $\lambda_i = 0$ and ending at $\lambda_f = \pi/2$, where $\epsilon_{\mathbf{r}, i}$ and $\epsilon_{\mathbf{r}, f}$ are independent and distributed uniformly on $[-W/2, W/2]$. Note that this is the same parametric evolution as in the case of the RMT protocol (4) but now with randomness only encoded in the on-site energies and hopping terms making it more feasible for experimental realizations.

In the case of the 'potential model' we consider the following Hamiltonian:

$$H_{\text{pot}}(\lambda) = -J \sum_{\mathbf{r}, \delta, \alpha, \alpha'} t_{\mathbf{r}, \delta, \alpha, \alpha'} |\mathbf{r} + \delta, \alpha\rangle \langle \mathbf{r}, \alpha'| + \sum_{\mathbf{r}, \alpha} (V_{\mathbf{r}, \lambda} + \epsilon_{\mathbf{r}}) |\mathbf{r}, \alpha\rangle \langle \mathbf{r}, \alpha| + \text{h. c.} \quad (6)$$

where level dynamics is now generated by the compression (decompression) of a parabolic potential, $V_{\mathbf{r}, \lambda} = \frac{1}{2} \frac{V_0}{L^2} (r^2 + \lambda (x^2 - y^2))$, in the x (y) direction in a symmetric way with λ starting at $-\lambda_f/2$ and ending at $\lambda_f/2$. Here, choosing the same $t_{\mathbf{r}, \delta, \alpha, \alpha'}$ hopping terms and on-site energies as in the on-site model (5), statistical properties of level dynamics are expected to be identical to the proper random matrix ensembles (i.e. unit, random phase and random SU(2) phase hoppings implying GOE, GUE and GSE-like behavior, respectively), albeit under slightly different conditions due to the presence of the confining potential.

III. LEVEL DYNAMICS

In this section we present our results on the level dynamics regarding the distribution of distance between adjacent levels, level velocities and level curvatures.

A. Level spacing statistics

In this subsection we investigate and compare the distribution of level spacing in the potential model to the RMT predictions. Previous thorough studies considered level spacing statistics with on-site disorder, and unit and random phase hoppings for the GOE and GUE symmetry classes, respectively [7, 10, 15] in 2 dimensions and almost perfect agreement was found with the Wigner-Dyson distribution (3) for energy eigenstates with localization lengths, ξ , much larger than the system size, $\xi \gg L$, (i.e. approximately uniform spatial eigenstate distribution). Furthermore, there is a true localization-delocalization transition in the presence of random spin-orbit coupling for the GSE ensemble [8, 16–19]. As disorder increases, however, the window of the RMT-like states gets narrower around the middle of the spectrum (extended states or states with localization length much larger than the system size), until the localization lengths of levels with energies closest to zero become comparable to the system size. Then in the opposite limit, as disorder is increased further, levels become completely uncorrelated and spacing statistics becomes Poissonian, $P_{\text{level}, \beta} \sim e^{-\Delta}$, as expected.

Analogously, both the uncorrelated, Poissonian, and the Wigner type regimes are present in the potential model, (6) but with the location of the RMT window dramatically affected by the potential. Qualitatively, the total band width stretches with increasing potential strength in a way that the lowest energy remains approximately at the value without potential, $\sim -2J - W$, and all excited states get lifted (throughout this paper we set the chemical potential to zero). This also implies a shift of the RMT window towards the lower edge of the energy band, i.e. at filling factors $f < 1/2$ with f denoting the ratio of the level at which the statistics is investigated and the total number eigenstates. These effects are demonstrated in Fig. 1 for the GUE ensemble, i.e. the stronger the potential the lower the filling factor at which levels display WD statistics and at half-filling Poissonian statistics is observed. Further increasing the potential, however, the RMT window reaches the lowest lying energy states, happening approximately for potential strengths comparable to the band width, $V_0 \sim L^2 J$. At this point no WD statistics is observable in the spectrum and the distribution of level spacing converges towards the uncorrelated Poissonian character both with increasing disorder and potential strength. This also implies that in the potential model in the case of RMT-like states potential effects can be neglected for not too large $\lambda < 1$ deformations as they always come up in form of

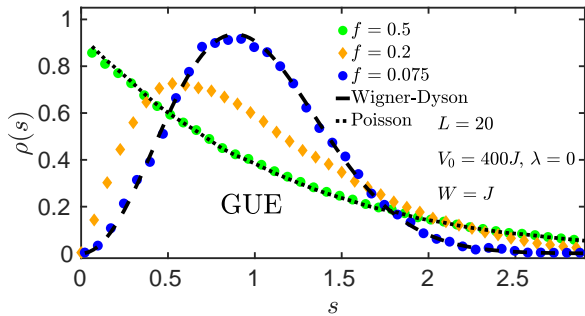


FIG. 1. Level spacing statistics in the potential model for the GUE ensemble for system size $L = 20$, disorder strength $W = J$ and potential strength $V_0 = 400J$ at $\lambda = 0$ for different filling factors, $f = 0.5, 0.2, 0.075$ (symbols). While for half-filling Poissonian statistics is displayed (dotted line), upon decreasing the filling factor (at $f = 0.075$) WD statistics is recovered up to high precision (dashed line).

$\lambda V_0/L^2$ contributing only as a subleading term compared to the symmetric point of $\lambda = 0$.

Let us further emphasize that the presence of the confining potential has a remarkable impact on the Anderson transition point in the GSE ensemble. For large enough potential strengths no localization-delocalization transition is observable as the value of the critical disorder ($W_c \approx 8.55$ for $V_0 = 0$) converges to zero upon increasing the potential strength. This effect is demonstrated in Fig. 2 for different potential strengths and degrees of deformation at half filling, where level statistics exhibits relevant deviations from WD statistics and a clear convergence towards Poissonian distribution, even for disorder strengths well below W_c . For better comparability in the figures, numerical data were scaled to have unit mean and plotted as a function of $s = \Delta/\langle\Delta\rangle$.

B. Level velocity statistics

Next we discuss the statistical properties of energy level velocities defined as the first derivative with respect to the parameter λ , i.e. the fictitious time in level dynamics. A simple expression is provided via first order perturbation theory:

$$v_n \equiv \frac{dE_n}{d\lambda} = \langle \varphi_{n,\lambda} | dH(\lambda) / d\lambda | \varphi_{n,\lambda} \rangle \quad (7)$$

with $|\varphi_{n,\lambda}\rangle$ denoting the n th instantaneous eigenstate at parameter value λ . Although in theory velocity can depend on the actual value of λ , for the RMT protocol (4) it is described by the same Gaussian statistics as the diagonal matrix elements of the given random ensemble for all instantaneous eigenstates, $\mathcal{P}(v_n) \sim e^{-\frac{\beta N}{4} v_n^2}$.

In the on-site model, (5) we observe Gaussian velocity statistics for levels with localization lengths much larger

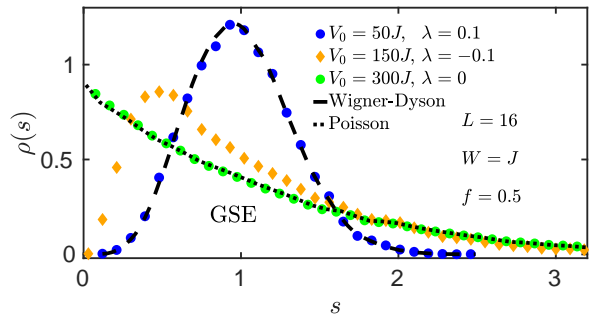


FIG. 2. Level spacing statistics in the potential model for the GSE ensemble for system size $L = 16$, disorder strength $W = J$, filling factor $f = 0.5$, potential strengths and deformations, $V_0 = 50J, 150J, 300J$, $\lambda = 0.1, -0.1, 0$, respectively (symbols). Although being far below the critical disorder at half-filling, level statistics starts to deviate from WD character (dashed line) and converges to a Poissonian distribution (dotted line) for $V_0 = 300J$.

than the system size in the limit of $1 \ll L \ll \xi$ or for delocalized eigenstates (GSE case). In this RMT-like regime eigenstate components are uniformly distributed on a βL^2 dimensional sphere with absolute value squares becoming independent identically distributed random variables with mean $1/L^2$ in the limit $L \gg 1$. Consequently, level velocity in (7) is given by a sum of independent identically distributed random variables as

$$v_n = \sum_{\mathbf{r}} |\varphi_{n,\lambda}(\mathbf{r})|^2 \partial_{\lambda} \varepsilon_{\mathbf{r},\lambda} \quad (8)$$

with the shorthand notation $\partial_{\lambda} \varepsilon_{\mathbf{r},\lambda} = -\varepsilon_{\mathbf{r},i} \sin \lambda + \varepsilon_{\mathbf{r},f} \cos \lambda$ having variance $W^2/12$ and $\varphi_{n,\lambda}(\mathbf{r}) = \langle \mathbf{r} | \varphi_{n,\lambda} \rangle$ with $\langle \mathbf{r} |$ denoting the \mathbf{r} th coordinate eigenstate.

Since $\partial_{\lambda} \varepsilon_{\mathbf{r},\lambda}$ is independent of $\varepsilon_{\mathbf{r},\lambda}$ and so of $|\varphi_{n,\lambda}(\mathbf{r})|^2$ as well, each term's variance scales as $\sim W^2/L^4$. Invoking the Central Limit Theorem all terms in the sum are independent giving a total variance of $\sim W^2/L^2$ and a Gaussian velocity statistics independent of the underlying symmetry class, $P(v) \sim e^{-v^2 L^2 / (2c_v W^2)}$, with c_v being some numerical constant originating from the variance of the eigenstate components and on-site energies. In the opposite, localized limit, however, eigenstate components get strongly correlated breaking down the above reasonings, displaying curves completely different from Gaussian and neither following the exact formula derived in Ref. 57. In addition, we find that Gaussian velocity statistics survives for slightly larger disorder strengths where clear deviations are already present in the level statistics. For instance, in the GOE case for $L = 25$ deviations from Gaussian velocity statistics only appear around $W \approx 10J$, while the threshold lies around $W \approx 2J$ in the case of level statistics. The above properties are demonstrated, for the sake of better comparability with the variances scaled to unity, in Fig. 3 together with the numerical verification of the disorder dependence of the variances.

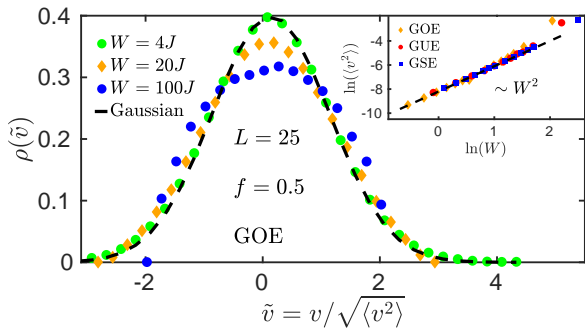


FIG. 3. Numerical results of the level velocity distribution for the on-site model in the case of the GOE ensemble for disorder strengths $W = 4J, 20J, 100J$, system size $L = 25$ and filling factor $f = 0.5$ (symbols). Numerical data were scaled such that all curves have unit variance for better comparability and shows perfect agreement with the standard Gaussian distribution for not too large on-site variances (dashed line). Increasing disorder induces deviations from Gaussian shape. Inset: Universal velocity variance for all the three ensembles following the same curve scaling as $\sim W^2$.

Turning to the potential model, characteristics similar to level spacing statistics are found. Namely, for the RMT-like energy states (either with localization length much larger than the system size or delocalized states in the GSE case), statistics of level velocities follow a Gaussian distribution up to high precision along with the same additional constraints as in the case of level statistics due to the potential. Note that now the mean of the velocity, in contrast to the RMT and on-site results, takes finite values growing linearly with λ and for finite values of λ it also increases with the potential strength. Nevertheless, most of the other statistical properties remain the same as for RMT-like states and for $\lambda < 1$ effects of the asymmetric potential appear only as subleading corrections of order $\sim \lambda V_0/L^2$ compared to the $\lambda = 0$ symmetric case. Considering first the variance of the velocity, it can easily be seen that it is independent of the disorder strength, as in the defining expression

$$v_n = \frac{V_0}{2L^2} \sum_{\mathbf{r}} |\varphi_{n,\lambda}(\mathbf{r})|^2 (x^2 - y^2) \quad (9)$$

only $|\varphi_{n,\lambda}(\mathbf{r})|^2$ is of statistical nature which, however, does not depend on the on-site variances in the RMT regime. Investigating further Eq. (9), one can deduce that its variance does not depend on the system size up to leading order either. The variance of the velocity can be expressed as

$$\begin{aligned} \langle v_n^2 \rangle &\sim L^{-4} \sum_{\mathbf{r}} \langle |\varphi_{n,\lambda}(\mathbf{r})|^4 \rangle (x^2 - y^2)^2 \\ &+ L^{-4} \sum_{\mathbf{r} \neq \mathbf{r}'} \langle |\varphi_{n,\lambda}(\mathbf{r})|^2 |\varphi_{n,\lambda}(\mathbf{r}')|^2 \rangle ((x')^2 - (y')^2) (x^2 - y^2). \end{aligned} \quad (10)$$

Here $(x^2 - y^2)$ and the $\sum_{\mathbf{r}}$ summations give $\sim L^2$ con-

tributions while the two averages scale as $\sim L^{-4}$. The first term then gives $J^2 L^{-4} L^{-4} L^6 \sim J^2 L^{-2}$ and the second one $\sim O(J^2)$ as there two summations are performed verifying that velocity variances are size independent up to leading order. In contrast to the on-site model, (9) is a sum of correlated random variables with different variances due to the inhomogeneity induced by the confining potential. Nevertheless, the general form of the Central Limit Theorem can still be applied implying again Gaussian statistics as each terms' variance and all correlations are negligibly small compared to the total variance. This latter can be easily seen as the total variance does not depend on L while the single variances can be upper bounded as $\langle |\varphi_{n,\lambda}(\mathbf{r})|^2 |\varphi_{n,\lambda}(\mathbf{r}')|^2 (x^2 - y^2) ((x')^2 - (y')^2) \rangle / L^4 < L^{-2} L^{-2} L^2 L^2 L^{-4} < L^{-4}$. In addition, we again find that the typical velocity magnitude does not depend on the parameter β in the RMT regime. Thus we conclude that in the potential model, in leading order and independently of the symmetry class, velocity variances remain constant, $\langle v^2 \rangle \sim O(J^2)$ with $\sim L^{-2}$ and $\sim \lambda V_0/L^2$ correction terms.

Summarizing our results, in the two models the following typical velocity magnitudes are observed:

$$\langle v^2 \rangle_{\text{on-site}} \sim W^2/L^2, \quad \text{independent of } \beta, \quad (11)$$

$$\langle v^2 \rangle_{\text{pot}} = O(J^2) + o(L^{-2}) + o(\lambda V_0/L^2), \quad (12)$$

independent of W and β .

Furthermore, for the GOE and GSE ensembles deviations from Gaussian statistics happen for slightly smaller values of V_0 than in the case of the GUE class. Our results (again with their variances scaled to unity for better comparability) are demonstrated in Fig. 4 for increasing values of the potential strength, different degrees of deformations and filling factors with the inset numerically

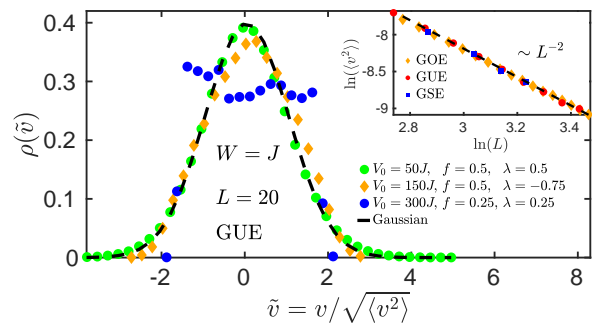


FIG. 4. Numerical results of the level velocity distribution for the potential model in the case of the GUE ensemble for potential strengths $V_0 = 50J, 150J, 300J$, filling factors $f = 0.5, 0.5, 0.25$ and deformations $\lambda = 0.5, -0.75, 0.25$, respectively, disorder strength $W = J$ and system size $L = 20$ (symbols). Curves scaled to have unit variances are in good agreement with the standard Gaussian distribution (dashed line) for not too large potential strengths. Inset: Universal velocity variance for all the three ensembles in the on-site model, decaying as $\sim L^{-2}$.

verifying the J^2L^{-2} scale of the variance in the on-site model.

C. Level curvature statistics

Turning to the curvature of energy levels, characterized by the second derivative with respect to λ , a compact expression is provided by second order perturbation theory:

$$\begin{aligned} K_n &\equiv \frac{d^2 E_{n,\lambda}}{d\lambda^2} \\ &= \langle \varphi_{n,\lambda} | d^2 H / d\lambda^2 | \varphi_{n,\lambda} \rangle + 2 \sum_{m \neq n} \frac{|\langle \varphi_{n,\lambda} | dH/d\lambda | \varphi_{m,\lambda} \rangle|^2}{E_{n,\lambda} - E_{m,\lambda}} \end{aligned} \quad (13)$$

with $|\varphi_{n,\lambda}\rangle(E_{n,\lambda})$ and $\langle \varphi_{n,\lambda}|(E_{n,\lambda})$ denoting again the instantaneous eigenstates (eigenvalues). Note that for both the RMT (4), and the on-site protocols (5), K_n is independent of the the actual value λ . In the case of the potential model, we concentrate again on the symmetric point of $\lambda = 0$ as for not too large deformations, $\lambda < 1$, there are no essential differences in the statistical properties of energy level curvatures as potential term corrections would only appear in form of $\lambda V_0/L^2$.

Following the strategy of Refs. 43 and 44, we restricted our investigation to levels around zero energy and computed numerically the second derivative of the energy levels being closest to zero at $\lambda = 0$. While in the on-site model, (5) and RMT the first term in (13) becomes $-E_{n,0}$ and so can be neglected, in the potential model (6) it is exactly zero as $d^2 H_{\text{pot}}/d\lambda^2 = 0$. In the same limits as before (long localization length or delocalized states), similarly to the previous subsection, curvature statistics in both the on-site and the potential model are in good agreement with the distribution derived in Refs. 43 and 44 for the RMT protocol, (4), and for disordered systems pierced through by an Aharonov-Bohm flux in Ref. 45. Their results state that the statistics follow up to high precision the generalized Cauchy distribution:

$$P(K) = \frac{C_\beta(W, L, V_0)}{(1 + K^2/\gamma^2(W, L, V_0))^{\beta/2+1}} \quad (14)$$

with C_β and γ being the normalization constant and the variance of the curvature, respectively, which can, in theory, depend on the system size, disorder and in our case also on the potential strength. In Refs. 43 and 44 it was shown that the curvature variance in RMT varies as $\gamma = \beta\pi\langle v^2 \rangle / \delta\epsilon$ (where $\delta\epsilon$ denotes the average mean level spacing around zero energy) and so the scaled, $k = \frac{K\delta\epsilon}{\pi\beta\langle v^2 \rangle}$ curvature yields universal statistics with C_β depending only on the symmetry class. In contrast, in our models we experience slight deviations from this universality, most probably due to the effects of the localized states outside of the region of RMT-like states contributing also to the sum in Eq. (13).

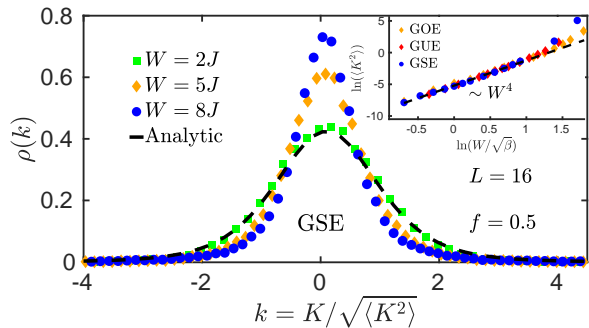


FIG. 5. Results on the level curvature distribution in the on-site model for the GSE ensemble with disorder strengths $W = 2J, 5J, 8J$, system size $L = 16$ and filling factor $f = 0.5$ (symbols). Numerical results agree well with the analytical predictions (dashed line) only below a slightly smaller threshold variance than in the case of level velocities. Inset: curvature variances collapsing onto a universal curve for all the three ensembles and following the observed $\sim W^4/\beta^2$ power-law behavior.

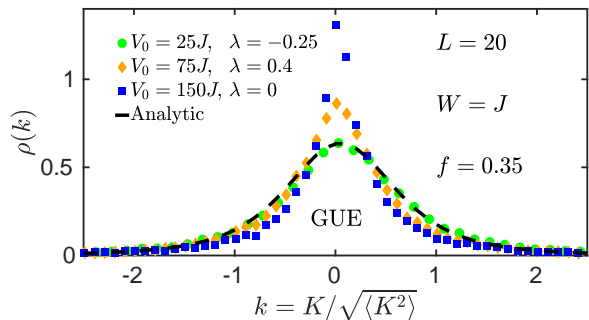


FIG. 6. Level curvature distribution in the potential model for the GUE ensemble for potential strengths $V_0 = 25J, 75J, 150J$ and deformations $\lambda = -0.25, 0.4, 0$, respectively, disorder strength $W = J$, system size $L = 20$ and filling factor $f = 0.35$ (symbols). Clear deviations are present even for $V_0 = 75J$ as a consequence of potential induced localization effects outside of the region of RMT-like states, while for smaller V_0 analytic predictions are in good agreement with numerical results (dashed line).

To this end we analyzed how the variances change with the disorder and the system size and found that in the on-site model, quite unexpectedly, the variance approximately scales as $\langle K^2 \rangle \sim W^4/J^2$, while it does not depend on the system size in the RMT-like regime. The latter can easily be understood as the numerator scales similarly as the velocity variance, $\sim J^2L^{-2}$, while the denominator's size dependence is trivially proportional to the inverse of the number of levels, $\sim JL^{-2}$. In the case of the potential model, somewhat surprisingly, we observe neither disorder nor size dependence up to leading order (comprehensively, only in the large localization length or delocalized regimes). In both models, moreover, the typical magnitude of the curvatures scales linearly with β . This

feature originates from the fact that while both the numerator (as it behaves similarly to the variance of level velocity) and the energy difference in the denominator are independent of β , the number of terms in the summation grows linearly with β . In total we obtain the following scales for the magnitude of level curvature captured by their variances:

$$\langle K^2 \rangle_{\text{on-site}} \sim \beta^2 W^4 / J^2, \text{ independent of } L \quad (15)$$

$$\langle K^2 \rangle_{\text{pot}} \sim \beta^2 O(J^2) + o(\lambda V_0 / L^2), \quad (16)$$

independent of W and L

As a further consequence of localized states further from zero energy manifests in the fact that the curvature distribution is much more sensitive to both the disorder and the potential strength. For the GSE ensemble, for instance, even for $W = 5J < W_c = 8.55J$ for system size $L = 16$, while for the GUE case for $V_0 = 75J$ relevant deviations are observable, as demonstrated in Figs. 5 and 6, respectively, again with variances scaled to unity with the inset in Fig. 5 providing numerical verification of the observed $\sim W^4 / \beta^2$ universal power-law behavior.

IV. STATISTICS OF AVOIDED LEVEL CROSSINGS

In this section we turn to the discussion of the statistics of the LZ parameters, i.e. the gap and asymptotic slope of energy levels at the avoided level crossings. In systems with no particular symmetries single parameter variations in random Hamiltonians induce avoided crossings, neighboring levels approaching very closely to each other, but finally avoiding true degenerate points. Such an anticrossing, located at λ_0 , can be described by the effective 2×2 matrix, in the limit that the separation from the other levels are much larger than the typical distance between the two energies:

$$H = \begin{bmatrix} \lambda\gamma/2 & \Delta_{\min} \\ \Delta_{\min} & -\lambda\gamma/2 \end{bmatrix}, \quad (17)$$

$$\Delta(\lambda) = E_+(\lambda) - E_-(\lambda) = \sqrt{\Delta_{\min}^2 + \gamma^2(\lambda - \lambda_0)^2} \quad (18)$$

with E_{\pm} , Δ_{\min} and γ denoting the two eigenvalues, the gap and the asymptotic slope, respectively.

In the case of random matrices, concentrating on the middle of the energy spectrum, statistics of Δ and γ were calculated by Wilkinson in Refs. 71 and 72 for the protocol Eq. (4) when the value of λ is changed from 0 to $\pi/2$:

$$\rho_{\beta}(\tilde{\Delta}_{\min}) \sim \tilde{\Delta}^{\beta-1} e^{-C_{\beta,\Delta} \tilde{\Delta}_{\min}^2}, \quad (19)$$

$$\rho_{\beta}(\tilde{\gamma}) \sim \tilde{\gamma}^{\beta+1} e^{-C_{\beta,\gamma} \tilde{\gamma}^2}, \quad (20)$$

with $C_{\beta,\Delta} = \frac{1}{\sqrt{\pi}}, \frac{\pi}{4}, \frac{9\pi}{16}$ and $C_{\beta,\gamma} = \frac{4}{\pi}, \frac{9\pi}{64}, \frac{225\pi}{256}$ for GOE, GUE and GSE, respectively and where

we introduced the following dimensionless quantities $\tilde{\Delta}_{\min} \equiv \Delta_{\min} / \langle \Delta_{\min} \rangle$, $\tilde{\gamma} \equiv \gamma / \langle \gamma \rangle$ chosen such that the statistics have unit mean. Note that for both cases the distributions are independent and follow different curves for the symmetry classes $\beta = 1, 2, 4$, respectively.

To this end we collected numerical data of the Landau-Zener parameters for several disorder realizations between the levels around the zero energy states (i.e. the middle of the spectrum in the on-site model and RMT) and compared the obtained statistics scaled to unit mean values to the RMT results. Our results demonstrate that in similar limits as in the previous sections gap and slope statistics follow the predicted analytic formulas up to high precision. As far as their sensitivity to localization is concerned, while gap statistics behave similarly to level spacing statistics, slope statistics show patterns similar to level velocity statistics. In agreement with this latter statement, slope scales with the disorder strength and the system size exactly the same way as it was observed for the level velocities, i.e. in the on-site model $\langle \gamma \rangle \sim WL^{-1}$, while it is independent of both parameters in the case of the potential model and it does not depend on the particular ensemble either up to leading order. Note that both parameters can only take positive values so it is satisfactory to consider their mean values instead of their variances. Regarding further the typical magnitude of the gaps we observe that it scales with the system size as $\langle \Delta_{\min} \rangle \sim JL^{-2}$ in both models, as expected, while quite surprisingly it is insensitive to the disorder strength up to numerical precision. Remarkably it also implies that, in strong contrast to RMT, the gap is not proportional to the mean level spacing (for RMT-like states) which latter does increase with the disorder strength.

Next we turn to the analysis of the typical spacing, $\Delta\lambda$, between adjacent anticrossings and the typical width, $\delta\lambda$, of them, i.e. the approximate region where the formula Eq. (17) holds up to good precision. As pointed out in Refs. 71–78, in slowly driven disordered systems, where RMT description is applicable for the instantaneous energy spectrum, dynamics is very well captured by classical diffusion of hardcore particles in energy space, where transitions happen at the avoided level crossings, approximately around the $\delta\lambda$ region of the closest approach. Furthermore, of utmost importance is its relation to the typical spacing between adjacent avoided crossings providing information about the geometrical structure or "typical shape" of the anticrossings. While, comprehensively, the typical width should scale as the ratio of the gap and the slope,

$$\delta\lambda \sim \frac{\langle \Delta_{\min} \rangle}{\langle \gamma \rangle}, \quad (21)$$

the typical spacing is captured by counting the average number of the avoided crossings, N_{cross} , being inversely proportional to the spacing, $\Delta\lambda \sim N_{\text{cross}}^{-1}$. In RMT we previously showed [76] that the average number grows as $N_{\text{cross}} \sim \sqrt{N}$. Counting also the number of the anti-

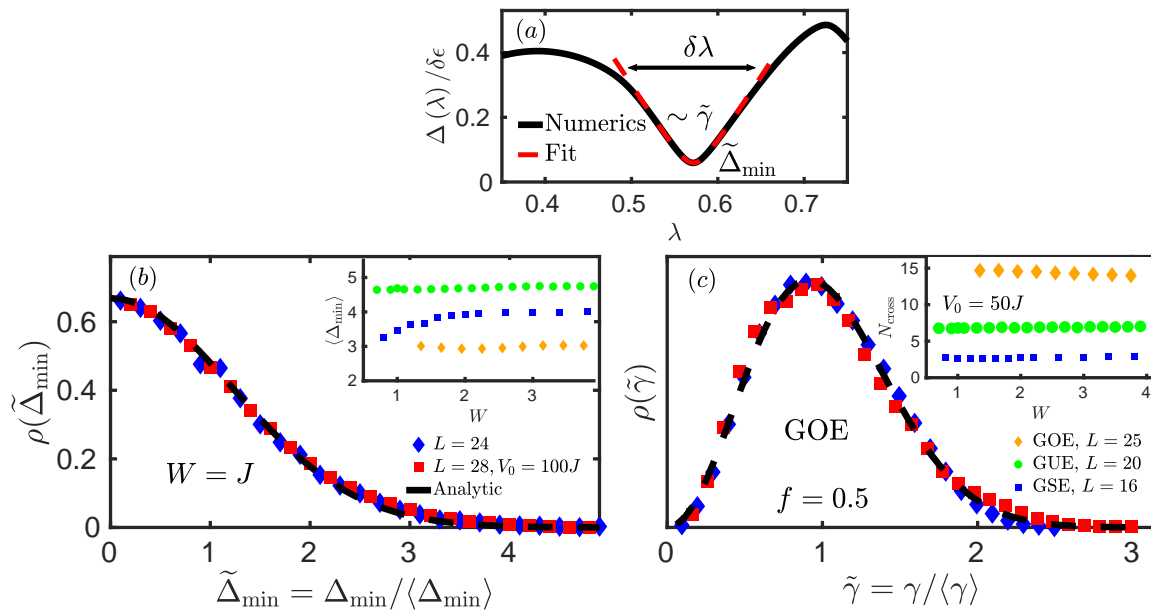


FIG. 7. Comparison of the distribution of the gap and the asymptotic slope at the avoided level crossings obtained in the two-dimensional models and the RMT analytical results for the GOE ensemble (symbols). (a): Typical shape of an avoided crossing with width $\delta\lambda$, slope $\tilde{\gamma}$ and gap $\tilde{\Delta}_{\min}$, with the dashed line fitting the Landau-Zener approximation of the level distance. (b): Gap distribution for the on-site and potential model. Red squares: potential model for system size, variance and potential strength, $L = 28$, $W = J$, and $V_0 = 100J$, respectively. Blue diamonds: on-site model results for $L = 24$ and $W = J$. Good agreement is observed with the analytical results (dashed line). Inset: Disorder dependence of the gap in the potential model for $V_0 = 50J$ showing insensitivity, up to numerical precision, for all the three ensembles. (c): Distributions of the asymptotic slope for the same parameters. Numerical data collected from around zero energy and scaled to have unit mean values are in good agreement with the RMT analytical results (dashed line). Inset: Disorder dependence of the number of the avoided level crossings in the potential model for $V_0 = 50J$, exhibiting again constant behavior up to numerical precision.

crossings while analyzing their LZ parameters we found that in the on-site model it also grows with the square root of the number of levels, $N_{\text{cross}} \sim L$, while in the potential model it increases linearly with the number of lattice sites, $N_{\text{cross}} \sim L^2$. As far as the disorder dependence is concerned, our numerical results show that, as one would expect, up to high precision no disorder dependence is observed in the potential model, while in the on-site model it grows as $N_{\text{cross}} \sim WJ^{-1}$. So in total we obtain for the parameters:

$$\Delta\lambda^{\text{pot}} \sim L^{-2}, \quad \Delta\lambda^{\text{on-site}} \sim JW^{-1}L^{-1}, \quad (22)$$

$$\langle\Delta_{\min}\rangle_{\text{pot}} \sim JL^{-2}, \quad \langle\Delta_{\min}\rangle_{\text{on-site}} \sim JL^{-2}, \quad (23)$$

$$\langle\gamma\rangle_{\text{pot}} \sim O(J), \quad \langle\gamma\rangle_{\text{on-site}} \sim WL^{-1}, \quad (24)$$

$$\delta\lambda_{\text{pot}} \sim L^{-2}, \quad \delta\lambda_{\text{on-site}} \sim JW^{-1}L^{-1}. \quad (25)$$

Thus we see that the "shape" or "geometry" of the anticrossings is invariant against disorder strength and system size as the ratio of the typical widths and typical spacings in both models is disorder and system size independent up to leading order (neglecting subleading $\sim \lambda V_0/L^2$ potential corrections), i.e. for $L \rightarrow \infty$ they neither disappear (limit of $\delta\lambda/\Delta\lambda \rightarrow 0$) nor merge together (limit of $\delta\lambda/\Delta\lambda \rightarrow \infty$):

$$\frac{\delta\lambda}{\Delta\lambda} \sim O(1). \quad (26)$$

We remark that although potential dependences can also arise, they always come up as $\lambda V_0/L^2$, which yields only a lower order contribution in comparison to the leading order of $O(1)$, as discussions of the preceding sections indicated that no RMT-like states can be found for $V_0 > L^2J$. The numerical verifications of our statements can be seen in Fig. 7 for the GOE ensemble showing the agreement of the gap and slope statistics with the analytical formulas [71, 72] and with the inset also displaying the disorder independence of the number and of the gap of the anticrossings for the potential model. Moreover, in Fig. 8 similar agreement is demonstrated for the LZ distributions in the case of the GUE and GSE ensembles with the insets verifying the size dependence of the number of the anticrossings for both models, the linear disorder strength scale of the number of the avoided crossings and the constant behavior of the gap for the on-site model.

The universal "geometry" of the avoided level crossings also implies universal (disorder and size independent) transition rates and single particle dynamics in the case of slow quantum quenches, once proper velocity and time scales are chosen. For the sake of simplicity consider linear time-evolution in parameter space, $\lambda(t) = \lambda_i + vt$, with transition probabilities at the avoided crossings

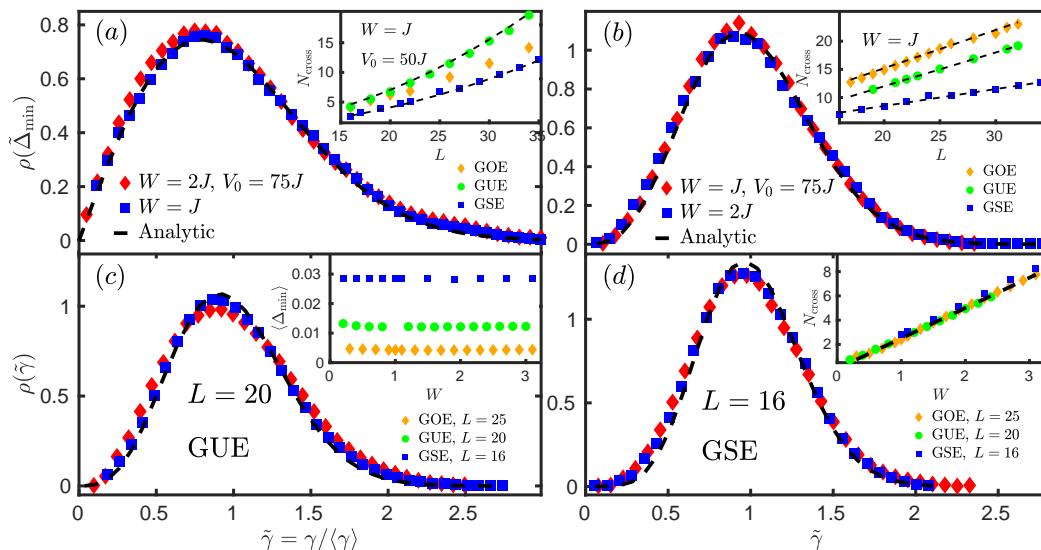


FIG. 8. Statistics of the Landau-Zener parameters at the avoided crossings for the GUE and GSE ensembles comparing the RMT numerical results with the on-site and potential model (symbols). (a): Gap distribution for the GUE ensemble for system sizes, disorder strengths and potential strengths, $L = 20$, $W = 2J$, J and $V_0 = 75J$ for the potential model and on-site model, respectively. Inset: Average number of the avoided level crossings in the potential model with $V_0 = 50J$ and $W = J$ as a function of the system size growing as $\sim L^2$ (dashed line) for all the three ensembles (b): Gap distribution for the GSE ensemble for parameters $L = 16$, $W = J, 2J$ and $V_0 = 75J$, respectively for the potential and the on-site model. In both cases remarkable agreement is observed with the RMT analytical results (dashed line). Inset: Average number of the anticrossings as function of the system size at $W = J$ for the on-site model growing linearly (dashed line). (c) and (d): Slope distributions for the same parameters, with the two disordered models following the same curves up to high precision (dashed line). Inset of (c): Scaling of the gap as a function of the disorder strength in the on-site model showing constant behavior up to numerical precision. Inset of (d): Average number of the avoided crossings for the on-site model growing linearly with the disorder strength (dashed line) and with approximately the same coefficient for all the three ensembles.

given by the celebrated Landau-Zener formula [69, 70]:

$$P_{LZ} = e^{-\frac{\pi}{2} \frac{\Delta_{\min}^2}{\gamma v}}. \quad (27)$$

Introducing, in the case of slowly driven, near adiabatic processes, dimensionless time and velocity, measured in units determined by the gap and frequency of the avoided crossings $\tilde{t} = t/t_c$, $t_c = 1/\langle\Delta_{\min}\rangle$, $\tilde{v} = v/v_c$, $t_c v_c = \Delta\lambda \Rightarrow v_c = \langle\Delta_{\min}\rangle\Delta\lambda$, leads to size and disorder independent Landau-Zener transition probabilities. To see this, consider the exponent of Eq. (27) which implies a velocity scale of $v_c = \frac{\langle\Delta_{\min}\rangle^2}{\langle\gamma\rangle}$ in order to have universal transition strengths, which using the relation $\delta\lambda \sim \frac{\langle\Delta_{\min}\rangle}{\langle\gamma\rangle}$ leads to

$$v_c = \frac{\langle\Delta_{\min}\rangle^2}{\langle\gamma\rangle} = \langle\Delta_{\min}\rangle\delta\lambda \sim \langle\Delta_{\min}\rangle\Delta\lambda, \quad (28)$$

where in the last step we used our knowledge about the fact that in both models, $\delta\lambda/\Delta\lambda$ is independent of both the system size and the disorder strength up to leading order. Moreover, for fixed dimensionless velocities and quench times we get the same number of the avoided crossings on average as well. Hence in slowly driven systems, where level-to-level transitions mostly happen at the anticrossings, on average the same number of such

transitions happen with the same strength (up to leading order in the potential model) implying universal single particle dynamics.

V. CONCLUSIONS

In this work we investigated the statistical properties of the dynamics of energy levels of disordered two-dimensional quantum dot models defined in Eqs. (5) and (6) and compared them to those of Random Matrix Theory. In the on-site (5) model, the same quench protocol was applied as in RMT, but with randomness only involved in the on-site energies with nearest neighbor hoppings, while in the potential model (6) with fixed on-site random energies and hopping terms the motion of the energy levels was generated by a parabolic potential compressed (decompressed) in the x (y) direction. First we considered the statistics of the distance, velocity and curvature of energy levels, as being relevant for analyzing chaotic nature in classical counterpart systems and determining responses of disordered nanosystems to external time-dependent perturbations. As for the level spacing distribution we found remarkable agreement between the two models and the RMT results for all the three ensembles (GOE, GUE, GSE) and discussed also the additional

localization effects induced by the confining potential. Next we verified within the regime of parameters where RMT-like states exist that the distributions of level velocity and level curvature follow up to high precision the RMT analytical curves and studied in detail their typical magnitudes as a function of the disorder strength and system size.

In the last section we investigated the statistical properties of the avoided level crossings, playing important role in near adiabatic non-equilibrium processes. In a similar way, almost perfect agreement was found between the RMT results and the disordered models. Considering the size and disorder dependences of the LZ parameters we found agreement for the gap for both the two-dimensional models and the RMT results scaling with the inverse of the number of energy levels while insensitivity to disorder strength was observed. For the slope and the average number of the avoided crossings, however, different scalings were observed. While the number of the avoided crossings was found to grow according to the square root of the system size for RMT and the on-site model, it scaled with the number of energy levels in the potential model. As far as the disorder dependence of the anticrossing number is concerned, in the on-site model linear growth, while in the potential model insen-

sitivity were observed up to numerical precision. For the scalings of the slope the same behavior was displayed as for the variance of the velocity statistics. Despite the different scalings, we concluded our discussion with the fact that the natural time and velocity units matched the ones predicted by size and disorder strength independent Landau-Zener transition rates, implying universal slowly driven dynamics.

Our findings for the level dynamics in two-dimensional disordered systems can be extended in many natural ways. To say the least, localization properties and spacing statistics of the Floquet eigenstates and quasi energies in cyclic drivings or criticality analysis of the instantaneous eigenstates at the localization-delocalization transition in the potential model for the GSE ensemble can also provide a fruitful perspective for future research.

ACKNOWLEDGMENTS

We thank Felix von Oppen for interesting discussions. This work was supported by the National Research, Development and Innovation Office (NKFIH) through the Hungarian Quantum Technology National Excellence Program, project no. 2017-1.2.1-NKP-2017- 00001.

-
- [1] E. P. Wigner, *Ann. Math.* **53**, 36 (1951); **62**, 548 (1955); 65, 203 (1957); 67, 325 (1958)
 - [2] O. Bohigas, in *Chaos and Quantum Physics*, edited by M. -J. Giannoni, A. Voros, and J. Zinn-Justin (Elsevier, Amsterdam, 1992)
 - [3] M. L. Mehta, *Random Matrices*, 2nd ed. (Academic, New York, 1991)
 - [4] C. W. J. Beenakker, *Rev. Mod. Phys.* **69**, 731 (1997)
 - [5] T. Guhr, A. Müller-Groeling, and H. A. Weidenmüller, *Phys. Rep.* **299**, 189-425 (1998)
 - [6] E. Hofstetter and M. Schreiber, *Phys. Rev. B*, **48**, 16979 (1993)
 - [7] M. Miller, D. Ullmo, and H. U. Baranger, *Phys. Rev. B*, **72**, 045305 (2005)
 - [8] S. N. Evangelou and T. Ziman, *J. Phys. C: Solid State Phys.*, **20**, L235-L240 (1987)
 - [9] S. N. Evangelou, *New J. Phys.*, **6**, 200 (2004)
 - [10] Kh. Zharekeshev, M. Batsch, and B. Kramer, *Europhys. Lett.*, **34** (8), 587-592 (1996)
 - [11] M. V. Berry and M. Tabor, *Proc. R. Soc. Lond. A*, **356**, 375-394 (1977)
 - [12] F. J. Dyson, *J. Math. Phys.* **3**, 140 (1962);
 - [13] B. I. Shklovskii, B. Shapiro, B. R. Sears, P. Lambrianides, and H. B. Shore, *Phys. Rev. B*, **47**, 11487 (1993)
 - [14] I. Kh. Zharekeshev, and B. Kramer, *Phys. Rev. Lett.*, **79**, 717 (1997)
 - [15] M. Batsch, L. Schweitzer, and B. Kramer, *Physica B*, **249**, 792 (1998)
 - [16] S. N. Evangelou, *Phys. B*, **39**, 12895 (1989)
 - [17] S. N. Evangelou, *Phys. Rev. Lett.*, **75**, 2550 (1995)
 - [18] T. Ando, *Surf. Science*, **196**, 120 (1988)
 - [19] Y. Asada and K. Slevin, *Phys. Rev. Lett.*, **89**, 25 (2002)
 - [20] Y. Alhassid and C. H. Lewenkopf, *Phys. Rev. Lett.*, **75**, 3922 (1995)
 - [21] M. V. Berry and M. Robnik, *J. Phys. A*, **19**, 649 (1986)
 - [22] N. Dupuis and G. Montambaux, *Phys. Rev. B*, **43**, 14390 (1991)
 - [23] F. Haake, M. Kus, and R. Scharf, *Z. Phys. B*, **65**, 381 (1987)
 - [24] Y. Avishai, J. Richert, and R. Berkovits, *Phys. Rev. B*, **66**, 052416 (2002)
 - [25] K. Kudo and T. Deguchi, *Phys. Rev. B*, **69**, 132404 (2004)
 - [26] R. Hamazaki and M. Ueda, *Phys. Rev. E*, **99**, 042116 (2019)
 - [27] M. Serbyn and J. E. Moore, *Phys. Rev. B*, **93**, 0414424 (R) (2016)
 - [28] A. Pandey, A. Kumar, and S. Puri, *Phys. Rev. B*, **101**, 022217 (2020)
 - [29] A. Kumar, A. Pandey, and S. Puri, *Phys. Rev. B*, **101**, 022218 (2020)
 - [30] C. Poli, G. A. Luna-Acosta, and H.-J. Stöckmann, *Phys. Rev. Lett.*, **108**, 174101 (2012)
 - [31] F. Haake, *Quantum Signatures of Chaos*
 - [32] P. Pechuka, *Phys. Rev. Lett.*, **51**, 943 (1983)
 - [33] T. Yukawa, *Phys. Rev. Lett.*, **54**, 1883 (1985)
 - [34] J. Edwards and D. J. Thouless, *J. Phys. C: Solid State Phys.*, **5**, 807 (1972)
 - [35] D. J. Thouless, *Phys. Rep.*, **13C**, 93 (1974)
 - [36] E. Akkermans and G. Montambaux, *Phys. Rev. Lett.*, **68**, 642 (1992)
 - [37] E. J. Austin and M. Wilkinson, *Nonlinearity*, **5**, 1137-1150 (1992)
 - [38] P. Gaspard, S. A. Rice, H. J. Mikeska, and K. Nakamura

- Phys. Rev. A, **42**, 4015 (1990)
- [39] J. Zakrzewski and D. Delande, Phys. Rev. E, **47**, 1650 (1993)
- [40] B. D. Simons, A. Hashimoto, M. Courtney, D. Kleppner, and B. L. Altshuler, Phys. Rev. Lett., **71**, 2899 (1993)
- [41] B. D. Simons and B. L. Altshuler, Phys. Rev. B, **48**, 5422 (1993)
- [42] B. D. Simons, A. Szafer, and B. L. Altshuler, Pis'ma Zh. Eksp. Tero. Fiz., **48**, 268-272 (1993)
- [43] F. v. Oppen, Phys. Rev. Lett., **73**, 798 (1994)
- [44] F. v. Oppen, Phys. Rev. E, **51**, 2647 (1995)
- [45] Y. V. Fyodorov and H.-J. Sommers, Phys. Rev. E, **51**, R2719(R) (1995)
- [46] Y. V. Fyodorov, H.-J. Sommers, Z. Physik B, **99**, 123 (1995)
- [47] D. Braun and G. Montambaux, Phys. Rev. B, **50**, 7776 (1994)
- [48] D. Braun, E. Hofstetter, A. MacKinnon, and G. Montambaux, Phys. Rev. B, **55**, 7557 (1997)
- [49] M. Barth, U. Kuhl, and H.-J. Stöckmann, Phys. Rev. Lett., **82**, 2026 (1999)
- [50] Y. Hlushchuk, U. Kuhl, and S. Russ, Phys. A: Stat. Mech., **3**, 344 (2004)
- [51] M. P. Pato, K. Schaadt, A. P. B. Tufaile, C. Ellegaard, T. N. Nogueira, and J. C. Sartorelli, Phys. Rev. E, **71**, 037201 (2005)
- [52] F. Simmel and M. Eckert, Phys. Rev. E, **51**, 5435 (1995)
- [53] H.-J. Stöckmann, M. Barth, U. Dörr, U. Kuhl, H. Schanze, Physica E, **9**, 571-577 (2001)
- [54] T. Takami and H. Hasegawa, Phys. Rev. Lett., **68**, 419 (1992)
- [55] G. Casati, I. Guarneri, F. M. Izrailev, L. Molinari, and K. Zyczkowski, Phys. Rev. Lett., **72**, 2697 (1994)
- [56] C. M. Canali, C. Basu, W. Stephan, and V. E. Kravtsov, Phys. Rev. B, **54**, 1431 (1996)
- [57] Y. V. Fyodorov, Phys. Rev. Lett., **73**, 2688 (1994)
- [58] I. Kh. Zharekeshv and B. Kramer, Physica A., **266**, 450 (1999)
- [59] D. Saher, F. Haake, and P. Gaspard, Phys. Rev. A, **44**, 7841 (1991)
- [60] M. Filippone, P. W. Brouwer, J. Eisert, and F. v. Oppen, Phys. Rev. B, **94**, 201112(R) (2016)
- [61] A. Maksymov, P. Sierant, and J. Zakrzewski, Phys. Rev. B, **99**, 224202 (2019)
- [62] C. Monthus, J. Phys. A: Math. Theor., **50**, 095002 (2017)
- [63] J. von Neumann and E. Wigner, Phys. Z. **30**, 467 (1929)
- [64] D. W. Noid, M. L. Koszykowski, and R. A. Marcus, Chem. Phys. Lett., **73**, 269 (1980)
- [65] D. W. Noid, M. L. Koszykowski, and R. A. Marcus, J. Chem. Phys., **78**, 4018 (1983)
- [66] B. Milek, W. Norenborg, and P. Rozemej, Z. Phys. A, **334**, 233 (1989)
- [67] T. Takami, Phys. Rev. Lett., **68**, 3371 (1992)
- [68] X. Yang, J. Burgdörfer, Phys. Rev. A, **48**, 83 (1993)
- [69] L. Landau, Phys. Z. Sowj., **2**, 46 (1932)
- [70] C. Zener, Proc. R. Soc., **137**, 696 (1932)
- [71] M. Wilkinson, J. Phys. A: Math. Gen. **22**, 2795 (1989)
- [72] P. N. Walker, M. J. Sánchez, and M. Wilkinson, J. Math. Phys. **37**, 5019 (1996)
- [73] M. Wilkinson, J. Phys. A: Math. Gen. **21**, 4021 (1988)
- [74] M. Wilkinson and E. J. Austin, J. Phys. A: Math. Gen. **28**, 2277 (1995)
- [75] M. Wilkinson, Phys. Rev. A **41**, 4645 (1990)
- [76] I. Lovas, A. Grabarits, M. Kormos, and G. Zaránd, Phys. Rev. Research, **2**, 023224 (2020)
- [77] A. Grabarits, M. Kormos, I. Lovas, and G. Zaránd, Phys. Rev. B, **106**, 064201 (2022)
- [78] A. Grabarits, M. Kormos, I. Lovas, and G. Zaránd, arXiv:2204.11627
- [79] M. Latka, P. Grigolini, and B. J. West, Phys. Rev. E, **50**, 596 (1994)
- [80] M. Latka, P. Grigolini, and B. J. West, Phys. Rev. E, **50**, 1073 (1994)
- [81] B. P. Holder and L. E. Reichl, Phys. Rev. A, **72**, 043408 (2005)
- [82] T. Timberlake and L. E. Reichl, Phys. Rev. A, **64**, 033404 (2001)
- [83] V. Ahlers, R. Zillmer, and A. Pikovsky, Phys. Rev. E, **64**, 03623 (2001)
- [84] F. J. Arranz, F. Borondo, and R. M. Bentio, J. Chem. Phys., **107**, 2395 (1997)
- [85] S. J. Wang and S. Y. Chu, Phys. Rev. A, **47**, 3546 (1993)
- [86] B. Dietz, A. Heine, A. Richter, O. Bohigas, and P. Leboeuf, Phys. Rev. E **73**, 035201(R) (2006)
- [87] C. Poli, B. Dietz, O. Legrand, F. Mortessagne, and A. Richter, Phys. Rev. E **80**, 035204(R) (2009)
- [88] J. Goldberg and W. Schweizer, J. Phys A: Math. Gen. **24**, 2785-2791 (1991)
- [89] J. Zakrzewski and D. Delande, Phys. Rev. E, **47**, 1665 (1993)
- [90] J. Zakrzewski and M. Kus, Phys. Rev. Lett., **67**, 2749 (1991)
- [91] S. Adam, M. L. Polianski, X. Waintal, and P. W. Brouwer, Phys. Rev. B **66**, 195412 (2002)
- [92] D. Tobe, M. Kohmoto, M. Sato, and Y.-S. Wu, Phys. Rev. B **75**, 245203 (2007)
- [93] M. Wilkinson and E. J. Austin, Phys. Rev. A, **46**, 2601 (1993)